Differentiation of pre-ablation and post-ablation late gadolinium-enhanced cardiac MRI scans of longstanding persistent atrial fibrillation patients

Yang, Guang, Zhuang, Xiahai, Khan, Habib, Haldar, Shouvik, Nyktari, Eva, et al.

Guang Yang, Xiahai Zhuang, Habib Khan, Shouvik Haldar, Eva Nyktari, Lei Li, Xujiong Ye, Greg Slabaugh, Tom Wong, Raad Mohiaddin, Jennifer Keegan, David Firmin, "Differentiation of pre-ablation and post-ablation late gadolinium-enhanced cardiac MRI scans of longstanding persistent atrial fibrillation patients," Proc. SPIE 10134, Medical Imaging 2017: Computer-Aided Diagnosis, 101340O (3 March 2017); doi: 10.1117/12.2250910

SPIE.

Event: SPIE Medical Imaging, 2017, Orlando, Florida, United States

Differentiation of Pre-Ablation and Post-Ablation Late Gadolinium-Enhanced Cardiac MRI Scans of Longstanding Persistent Atrial Fibrillation Patients

Guang Yang [†a,b], Xiahai Zhuang [†c], Habib Khan [a,b], Shouvik Haldar [a], Eva Nyktari [a], Lei Li [c], Xujiong Ye [d], Greg Slabaugh [e], Tom Wong [a], Raad Mohiaddin [a,b], Jennifer Keegan [‡a,b], and David Firmin [‡a,b]

[a] Cardiovascular Biomedical Research Unit, Royal Brompton Hospital, SW3 6NP, London, UK;
[b] National Heart & Lung Institute, Imperial College London, SW7 2AZ, London, UK;
[c] SJTU-CU International Cooperative Research Centre, Department of Engineering Mechanics, Shanghai Jiao Tong University, Shanghai, 200240, China;
[d] School of Computer Science, University of Lincoln, LN6 7TS, Lincoln, UK;
[e] Department of Computer Science, City University London, EC1V 0HB, London, UK.

ABSTRACT

Late Gadolinium-Enhanced Cardiac MRI (LGE CMRI) is an emerging non-invasive technique to image and quantify pre-ablation native and post-ablation atrial scarring. Previous studies have reported that enhanced image intensities of the atrial scarring in the LGE CMRI inversely correlate with the left atrial endocardial voltage invasively obtained by electro-anatomical mapping. However, the reported reproducibility of using LGE CMRI to identify and quantify atrial scarring is variable. This may be due to two reasons: first, delineation of the left atrium (LA) and pulmonary veins (PVs) anatomy generally relies on manual operation that is highly subjective, and this could substantially affect the subsequent atrial scarring segmentation; second, simple intensity based image features may not be good enough to detect subtle changes in atrial scarring. In this study, we hypothesized that texture analysis can provide reliable image features for the LGE CMRI images subject to accurate and objective delineation of the heart anatomy based on a fully-automated whole heart segmentation (WHS) method. We tested the extracted texture features to differentiate between pre-ablation and post-ablation LGE CMRI studies in longstanding persistent atrial fibrillation patients. These patients often have extensive native scarring and differentiation from post-ablation scarring can be difficult. Quantification results showed that our method is capable of solving this classification task, and we can envisage further deployment of this texture analysis based method for other clinical problems using LGE CMRI.

Keywords: Atlas Propagation, Multi-Scale Patch, Local Atlas Ranking, Whole Heart Segmentation, Texture Analysis, Cardiac MRI, Classification, Machine Learning, Computer-Aided Diagnosis, Medical Imaging Analysis, Image Processing

1. INTRODUCTION

Late Gadolinium-Enhanced Cardiac MRI (LGE CMRI) is a promising technique to identify pre-ablation native and post-ablation induced atrial scars. Compared to the current gold standard, i.e., electro-anatomical mapping (EAM), which is performed during an invasive electrophysiological (EP) study [1], LGE CMRI is non-invasive, uses no ionizing radiation, and has reported higher accuracy of localization of the atrial scars [2]. Although some studies have demonstrated that there is an inverse correlation between the enhanced atrial scarring regions extracted from the LGE CMRI and left atrial endocardial voltage obtained from the EAM, the reproducibility of these findings is still debatable [3]. This may be due, firstly, to the previous

Medical Imaging 2017: Computer-Aided Diagnosis, edited by Samuel G. Armato III, Nicholas A. Petrick,
Proc. of SPIE Vol. 10134, 101340O · © 2017 SPIE · CCC code: 1605-7422/17/$18 · doi: 10.1117/12.2250910

delineation of left atrium (LA) and pulmonary veins (PVs) anatomy relying on operators' manual drawing which is highly subjective [4]; and secondly, simple intensity based image features or volumetric ratio between enhanced and non-enhanced voxels are over-simplified for the quantification of the atrial scarring. We hypothesized that, first, the LA and PVs anatomy can be accurately determined via a multi-atlas propagation based fully-automated whole heart segmentation (WHS); and second, that texture analysis on the extracted LA wall and PVs can provide more robust features for the LGE CMRI images than simple intensity-based measures. We validated our method by using it to differentiate pre-ablation LGE CMRI scans from post-ablation ones in cases of long-standing persistent atrial fibrillation patients. Cross validation results on 20 LGE CMRI scans of longstanding persistent atrial fibrillation (AF) patients showed dramatic improvement on the classification accuracy. And we can envisage the application of this technique for other cardiovascular clinical studies using LGE CMRI particularly in patients that atrial fibrosis can be quantified.

2. METHODOLOGY

2.1 Multi-Atlas Propagation Based Fully-Automated Whole Heart Segmentation (WHS)

Visualization of atrial scarring is performed by superimposing the enhanced signals derived from an LGE CMRI acquisition onto a 3D model of the LA and PV anatomy derived from a CMRI roadmap acquisition. Delineation of the heart anatomy in the CMRI roadmap study is a very challenging task and has generally been done using manual drawing by experienced operators. This suffers from two major pitfalls: first, the procedure is time-consuming and second, the manual segmentation is subjective and might not be reproducible. To automate this procedure, co-registration and a multi-atlas propagation based segmentation (MAS) method was proposed to accomplish the task [5]. Previous studies have shown that the multi-atlas can be built from just labeling LA and PVs [6] or labeling all the whole heart substructures including four chambers, major vessels and PVs [5]. The former method might be easier for atlas construction, but the segmentation accuracy of LA and PVs anatomy could be sacrificed without considering variances and deformation of surrounding substructures [6]; therefore, whole heart substructures were used in our atlas construction. In this study, we developed a MAS technique followed by a multi-scale patch based label fusion (MSP-LF) [7]. The developed WHS technique was applied to our CMRI roadmap whole-heart acquisition, and the LA and PVs anatomy was extracted (Figure 1). As both CMRI roadmap and LGE CMRI sequences are ECG gated, we can apply the extracted LA and PVs segmentation from the CMRI roadmap directly on to the LGE CMRI images (Figure 1). Further refinement of the PVs segmentation might be achieved via prior information provided by contrast-enhanced MR angiography or manual editing; however, non-gated MR angiography can cause mis-registration to the ECG gated LGE CMRI and further complicate the segmentation procedure. In this study, we focused on a fully automated WHS method for the delineation of LA and PVs without further manual intervention.

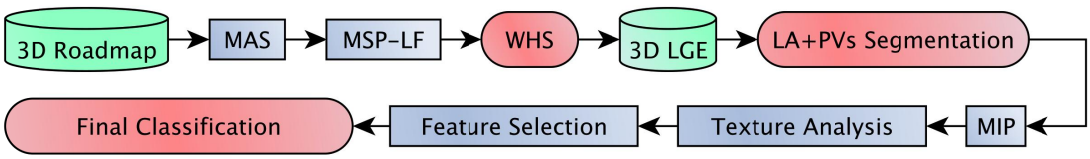

Figure 1: Flowchart of our fully automated WHS, texture analysis and classification workflow.

2.2 Maximum Intensity Projection and Feature Extraction via Texture Analysis

Following the WHS derived LA blood pool and PVs anatomy, we aim to extract information on possible atrial scarring in the LA wall and around PVs. Morphological dilation was applied to the derived LA blood pool and PVs to an extent of 3mm which is assumed to be the thickness of the LA wall [8]. Previous clinical-focused studies only considered intensity-based features, e.g., enhanced intensity or ratio between enhanced and overall LA wall and PVs regions [9].

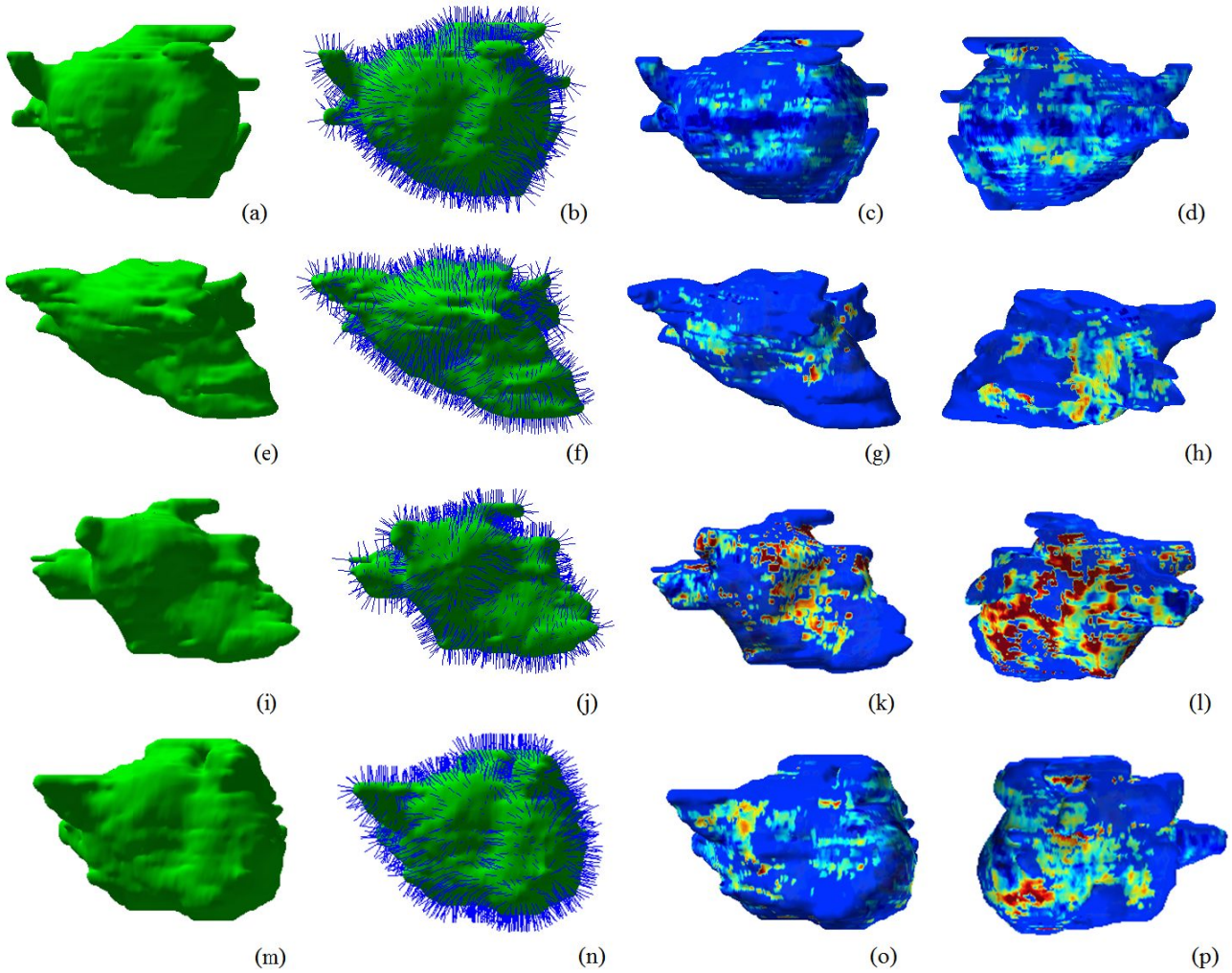

Figure 2: Visualization of the WHS results for two pre-ablation cases (a-d) and (e-h) and two post-ablation cases (i-l) and (m-p). First column: 3D surface rendering of the WHS results of LA and PVs; second column: the computed normals (blue lines) perpendicular to the segmented surface; Last two columns: anteroposterior and posteroanterior views of the 3D MIP showing the atrial scarring.

In this study, we employed texture based features for further quantification. Texture analysis has been successfully applied for the enhanced regions derived from LGE CMRI but for the infarction tissues in left ventricle only, which has much thicker myocardium [10]. It is very challenging to perform the texture analysis for the LA wall and PVs because the LA wall thickness is small and the voxel size is relatively large (1.5mm×1.5mm×4mm reconstructed to 0.75mm×0.75mm×2mm). Previous studies have used 3D maximum intensity projection (MIP, Figure 2) [6], and texture analysis can be performed after surface flattening [11];

however, this can introduce artifacts after interpolation. Considering previous limitations and challenges, we performed 2D MIPs for each WHS, with two projections being performed for each patient (from the central slice to the most superior and to the most inferior slices as shown in Figure 3 (a) and (b)). Multi-level Gabor wavelet filters based texture analysis has been adopted to extract robust image features (Figure 3 (c)) [12] and minimum redundancy maximum relevance (mRMR) was applied for further feature selection [12]. Ten selected texture features were used for the final classification task.

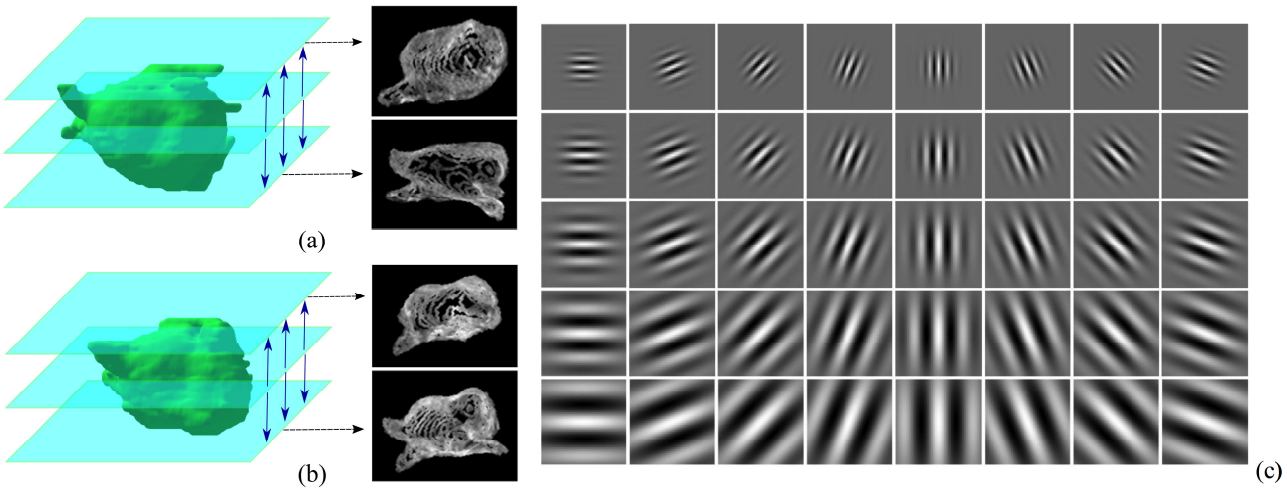

Figure 3: (a) Two 2D MIPs from the central slice to the most superior and to the most inferior slices for a pre-ablation case (blue arrows show the projection directions); (b) As (a) but applied for a post-ablation case; (c) Multi-level Gabor wavelet filters: 5 scales with 8 directions.

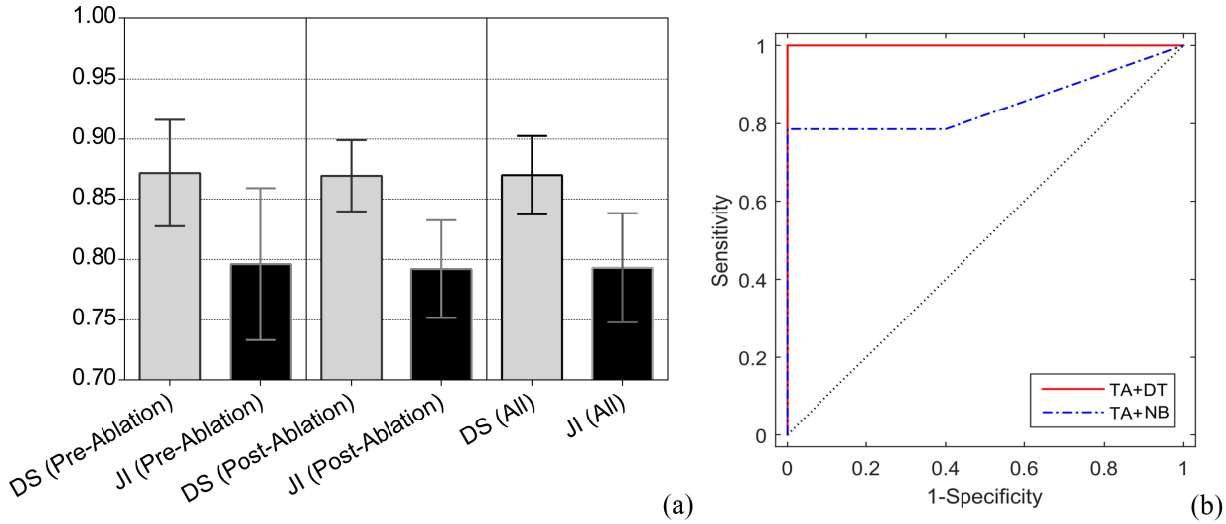

Figure 4: (a) WHS accuracy measured via Dice score (DS) and Jaccard Index (JI) for both pre-ablation cases, post-ablation cases and all the cases; (b) Comparison of the ROC for the texture analysis with naïve Bayes (TA+NB) or decision tree (TA+DT) classifiers.

2.3 Classification and Evaluation

The classification performance was evaluated by (i) Leave-One-Patient-Out (LOO) cross validation [13,14], which is an unbiased predictor and is capable of creating sufficient training data for studies with small sample size [14]; (ii) the area under the receiver operating characteristic (ROC) curve (AUC); (iii) the classification accuracy, sensitivity and specificity [15–17] at the operating point on the ROC curve using the both naïve Bayes (NB) [18,19] and decision tree (DT) based classifiers [20].

3. EXPERIMENTS AND RESULTS

We applied the classification and cross validation on 20 LGE CMRI scans of longstanding persistent AF patients. Figure 2 shows the 3D rendering of the WHS results (LA and PVs), and the 3D MIP of the enhanced atrial scarring. Figure 3 demonstrates the 2D MIP procedure and multi-level Gabor wavelet filters adopted. Figure 4 (a) summaries the accuracy of our WHS evaluated by both Dice score and Jaccard index. Figure 4 (b) shows the ROC curve of the classification results, and we compared the performance of using NB and DT based classifiers on texture features. We compared our method with using intensity based features: (i) using statistics (minimum, maximum, mean, median and standard deviation) extracted from image intensities of the segmented LA wall and PVs regions, and (ii) segmenting the enhanced scar regions using x-standard deviation method (x=2, 3, 4 or 6) [4], and the ratio between the enhanced volume and overall LA wall and PVs volume was then used as classification feature. According to a benchmark work [4], there is no significant difference obtained from various segmentation methods for atrial scarring delineation; therefore, in this work we used the classic standard deviation method to extract the atrial scarring and performed the comparison studies. Table 1 shows the comparison results of the classification using intensity based features and texture analysis derived features. LOO results showed that texture analysis with DT classifier achieved 100% accuracy, and significantly outperformed the results obtained by using the intensity based features.

Table 1: Quantitative results of the classification (IF+NB: intensity features with naïve Bayes classifier; IF+DT: intensity features with decision tree classifier; x-SD+NB: x-standard deviation and with naïve Bayes classifier; x-SD+DT: x-standard deviation and with decision tree classifier; TA+NB: texture analysis with naïve Bayes; TA+DT: texture analysis with decision tree classifier).

Method	Sensitivity	Specificity	PPV	NPV	Accuracy	AUC
IF+NB	40.00	93.33	66.67	82.35	80.00	0.67
IF+DT	40.00	86.67	50.00	81.25	75.00	0.75
2-SD+NB	40.00	93.33	66.67	82.35	80.00	0.37
2-SD+DT	40.00	100.00	100.00	83.33	85.00	0.52
3-SD+NB	40.00	100.00	100.00	83.33	85.00	0.40
3-SD+DT	40.00	100.00	100.00	83.33	85.00	0.53

Method	Sensitivity	Specificity	PPV	NPV	Accuracy	AUC
4-SD+NB	40.00	93.33	66.67	82.35	80.00	0.39
4-SD+DT	20.00	93.33	50.00	77.78	75.00	0.53
6-SD+NB	20.00	93.33	50.00	77.78	75.00	0.53
6-SD+DT	60.00	93.33	75.00	87.50	85.00	0.67
TA+NB	100.00	73.33	55.56	100.00	84.21	0.85
TA+DT	100.00	100.00	100.00	100.00	100.00	1.00

4. CONCLUSION

In this study, we proposed a fully automated workflow to process LGE CMRI images including objective delineation of LA and PVs anatomy and texture analysis based feature extraction. The designed workflow was applied to distinguish pre-ablation cases from post-ablation scans acquired by LGE CMRI. Such a task can be very difficult as all our patients suffered from longstanding persistent AF, and pre-ablation native atrial scarring can be quite extensive. We hypothesized that texture analysis can extract robust features for this challenging task subject to accurate anatomy segmentation. Our experimental results have

demonstrated the high efficacy of our workflow and we can expect our method to be deployed for other clinical problems using LGE CMRI. In particular, it may be able to improve the classification of patients pre-ablation, which is currently based on intensity based parameters which would provide increased guidance for the invasive ablation strategy.

REFERENCES

[1] Calkins, H., Kuck, K. H., Cappato, R., Brugada, J., Camm, A. J., Chen, S.-A., Crijns, H. J. G., Damiano, R. J., Davies, D. W., et al., "2012 HRS/EHRA/ECAS expert consensus statement on catheter and surgical ablation of atrial fibrillation: recommendations for patient selection, procedural techniques, patient management and follow-up, definitions, endpoints, and research trial design," Heart Rhythm 9(4), 632–696.e21 (2012).

[2] Ravanelli, D., Dal Piaz, E. C., Centonze, M., Casagranda, G., Marini, M., Del Greco, M., Karim, R., Rhode, K.., Valentini, A., "A novel skeleton based quantification and 3-D volumetric visualization of left atrium fibrosis using late gadolinium enhancement magnetic resonance imaging," IEEE Trans. Med. Imaging 33(2), 566–576 (2014).

[3] Harrison, J. L., Sohns, C., Linton, N. W., Karim, R., Williams, S. E., Rhode, K. S., Gill, J., Cooklin, M., Rinaldi, C. a., et al., "Repeat Left Atrial Catheter Ablation: Cardiac Magnetic Resonance Prediction of Endocardial Voltage and Gaps in Ablation Lesion Sets," Circ. Arrhythmia Electrophysiol. 8(2), 270–278 (2015).

[4] Karim, R., Housden, R. J., Balasubramaniam, M., Chen, Z., Perry, D., Uddin, A., Al-Beyatti, Y., Palkhi, E., Acheampong, P., et al., "Evaluation of current algorithms for segmentation of scar tissue from late gadolinium enhancement cardiovascular magnetic resonance of the left atrium: an open-access grand challenge.," J. Cardiovasc. Magn. Reson. 15, 105–122 (2013).

[5] Zhuang, X., Rhode, K. S., Razavi, R. S., Hawkes, D. J.., Ourselin, S., "A registration-based propagation framework for automatic whole heart segmentation of cardiac MRI," IEEE Trans. Med. Imaging 29(9), 1612–1625 (2010).

[6] Tao, Q., Ipek, E. G., Shahzad, R., Berendsen, F. F., Nazarian, S.., van der Geest, R. J., "Fully automatic segmentation of left atrium and pulmonary veins in late gadolinium-enhanced MRI: Towards objective atrial scar assessment.," J. Magn. Reson. Imaging 44(2), 346–354 (2016).

[7] Zhuang, X.., Shen, J., "Multi-scale patch and multi-modality atlases for whole heart segmentation of MRI," Med. Image Anal. 31, 77–87, Elsevier B.V. (2016).

[8] Knowles, B. R., Caulfield, D., Cooklin, M., Rinaldi, C. A., Gill, J., Bostock, J., Razavi, R., Schaeffter, T.., Rhode, K. S., "3-D visualization of acute RF ablation lesions using MRI for the simultaneous determination of the patterns of necrosis and edema," IEEE Trans. Biomed. Eng. 57(6), 1467–1475 (2010).

[9] Badger, T. J., Daccarett, M., Akoum, N. W., Adjei-Poku, Y. a., Burgon, N. S., Haslam, T. S., Kalvaitis, S., Kuppahally, S., Vergara, G., et al., "Evaluation of left atrial lesions after initial and repeat atrial fibrillation ablation; Lessons learned from delayed-enhancement MRI in repeat ablation procedures," Circ. Arrhythmia Electrophysiol. 3(3), 249–259 (2010).

[10] Kotu, L. P., Engan, K., Skretting, K., Måløy, F., Orn, S., Woie, L.., Eftestøl, T., "Probability mapping of scarred myocardium using texture and intensity features in CMR images.," Biomed. Eng. Online 12(1), 91 (2013).

[11] Karim, R., Ma, Y. L., Jang, M., Housden, R. J., Williams, S. E., Chen, Z., Ataollahi, A., Althoefer, K., Rinaldi, C. A., et al., "Surface flattening of the human left atrium and proof-of-concept clinical applications," Comput. Med. Imaging Graph. 38(4), 251–266, Elsevier Ltd (2014).

[12] Bonev, B., Escolano, F.., Cazorla, M., "Feature selection, mutual information, and the classification of high-dimensional patterns," Pattern Anal. Appl. 11(3–4), 309–319 (2008).

[13] Yang, G., Raschke, F., Barrick, T. R.., Howe, F. A., "Manifold Learning in MR Spectroscopy using Nonlinear Dimensionality Reduction and Unsupervised Clustering," Magn. Reson. Med. 74(3), 868–878 (2015).

[14] Yang, G., Raschke, F., Barrick, T. R.., Howe, F. A., "Classification of Brain Tumour 1H MR Spectra : Extracting Features by Metabolite Quantification or Nonlinear Manifold Learning?," Biomed. Imaging (ISBI), 2014 IEEE 11th Int. Symp. on. IEEE, 1039–1042 (2014).

[15] Soltaninejad, M., Ye, X., Yang, G., Allinson, N.., Lambrou, T., "An image analysis approach to MRI brain tumour grading," Oncol. News 9(6), 204–207 (2015).

[16] Soltaninejad, M., Ye, X., Yang, G., Allinson, N.., Lambrou, T., "Brain tumour grading in different MRI protocols using SVM on statistical features," Med. Image Underst. Anal., British Machine Vision Association (2014).

[17] Jones, T. L., Byrnes, T. J., Yang, G., Howe, F. A., Bell, B. A.., Barrick, T. R., "Brain tumor classification using the diffusion tensor image segmentation (D-SEG) technique," Neuro. Oncol. 17(3), 466–476, Oxford University Press (2014).

[18] Yang, G., Jones, T. L., Barrick, T. R.., Howe, F. A., "Discrimination between glioblastoma multiforme and solitary metastasis using morphological features derived from the p:q tensor decomposition of diffusion tensor imaging.," NMR Biomed. 27(9), 1103–1111 (2014).

[19] Murphy, K., Machine Learning: A Probabilistic Perspective, MIT Press (2012).

[20] Soltaninejad, M., Yang, G., Lambrou, T., Allinson, N., Jones, T. L., Barrick, T. R., Howe, F. A.., Ye, X., "Automated brain tumour detection and segmentation using superpixel-based extremely randomized trees in FLAIR MRI.," Int. J. Comput. Assist. Radiol. Surg. (2016).

† indicates corresponding authors G.Y. (g.yang@imperial.ac.uk) and X.H.Z. (zhuangxiahai@sjtu.edu.cn).
‡ indicates joint senior authors.

This study was funded by the British Heart Foundation Project Grant (Project Number: PG/16/78/32402) and the NIHR Cardiovascular Biomedical Research Unit, Royal Brompton Hospital & Harefield NHS Foundation Trust and Imperial College London. Data were obtained during the NIHR Efficacy and Mechanism Evaluation Programme (Project Number: 12/127/127).